UDK 539.412:621.791
Original scientific article/Izvirni znanstveni članek

ISSN 1580-2949
MTAEC9, 57(2)127(2023)

MECHANICAL AND METALLURGICAL PROPERTIES OF FRICTION-STIR-WELDED AISI 304 STAINLESS STEEL

MEHANSKE IN METALURŠKE LASTNOSTI TORNO VRTILNEGA VARJENJA NERJAVNEGA JEKLA AISI 304

Sundar raju Govindaraj*, Sivakumar Karuppan

Department of Mechanical Engineering, Bannari Amman Institute of Technology, Erode, Tamil Nadu, India

Prejem rokopisa – received: 2022-11-03; sprejem za objavo – accepted for publication: 2023-01-23

doi:10.17222/mit.2022.678

Friction stir welding of AISI 304 stainless-steel sheets was successfully carried out with a tungsten-alloy ($W+La_2O_3$) tool and the effect of the tool rotational speed on the microstructure and mechanical properties of the joints were evaluated. 3-mm-thick plates were friction-stir welded at various rotational speeds of 600–1000 min^{-1} and a constant welding speed of 40 mm/min with a constant axial load of 15 kN. Defect-free joints were produced at 800 min^{-1} and 900 min^{-1}, indicating a proper plastic flow of the material and ensuring adequate heat generation during welding. Tensile, Charpy impact, compression and microhardness tests were performed to evaluate the joint mechanical properties. The microstructural behavior of the welded and base-metal samples was examined with optical microscopy and scanning electron microscopy. According to the mechanical results, the welded material has a higher yield strength than the base metal due to the grain refinement and work hardening effect in the stir zone. FSW welds have a higher hardness than the base metal due to the high density of dislocations and continuous dynamic recrystallization. The joints also exhibit acceptable impact toughness. Finally, the EDS analysis confirms that there is no secondary-phase formation in the weld zone of the fabricated material.

Keywords: tensile strength, tool rotational speed, welding speed, axial load

V članku je opisano uspešno torno vrtilno varjenje oziroma varjenje s trenjem in mešanjem (FSW; angl.: Friction stir welding) pločevin iz nerjavnega jekla AISI 304. Varjenje so izvajali z orodjem iz volframa ($W+La_2O_3$) in so pri tem analizirali vpliv hitrosti vrtenja orodja na mikrostrukturo in mehanske lastnosti varjenih spojev. Jeklene pločevine debeline 3 mm so varili s postopkom FSW pri različnih hitrostih vrtenja orodja (od 600 do 1000) min^{-1} in pri konstantni hitrosti varjenja 40 mm/min s konstantno osno obremenitvijo 15 kN. Na ta način so uspeli izdelati zvarne spoje brez napak pri hitrostih 800 in 900 min^{-1} s primernim plastičnim tokom materiala in ustrezno tvorbo toplote zaradi trenja med varjenjem. Ovrednotili so mehansko kakovost izdelanih zvarnih spojev z nateznimi preizkusi, določitvijo Charpyjeve udarne žilavosti, tlačne trdnosti in meritvami mikrotrdote. Mikrostrukturo osnovnih pločevin in zvarnih spojev so analizirali s pomočjo svetlobnega in vrstičnega elektronskega mikroskopa. Na osnovi rezultatov mehanskih preiskusov so ugotavili, da imajo zvarni spoji v toplotno vplivaemn območju višjo mejo plastičnosti kot osnovni material zaradi udrobljenja kristalnih zrn in učinka deformacijskega utrjevanja v območju mešanja. S postopkom FSW izdelani zvarni spoji imajo višjo trdoto kot osnovni material zaradi večje gostote dislokacij in kontinuirne dinamične rekristalizacije. Zvarni spoji imajo prav tako sprejemljivo udarno žilavost. Poleg tega so analize EDS potrdile, da ni prišlo do tvorbe neželenih sekundarnih faz v območjih varjenja izbranega materiala.

Ključne besede: natezna trdnost, hitrost vrtenja orodja, hitrost varjenja, osna obremenitev

1 INTRODUCTION

Friction stir welding (FSW) is a solid-state joining technology developed in 1991 by the Welding Institute.[1] FSW is a hot working technique in which the workpiece is deformed severely by the rotating pin and shoulder.[2] The heat required to soften the material is generated by friction and plastic deformation.[3] Stainless steel fittings made of AISI 304 (UNS S30400/S30403) are reliable in a range of boating applications.[4] They are resistant to a wide range of climatic conditions and used for coastal handrails, hot-water pipes, and deck components for boats and ships.[5] Friction stir welding has been utilized on long straight welds used in the manufacture of pre-fabricated panels. In case of high melting temperature materials (HMT), FSW is considered more difficult to perform due to the tool wear and excessive frictional heat. It causes severe damage to the tool.[6] In particular, austenitic stainless steel endures high deformation at high temperatures.

The use of tools for the FSW of stainless steel alloys is problematic as it is difficult to retain the tool strength at high temperatures. The weld durability and quality are directly impacted by the tool selected. For this reason, the polycrystalline cubic boron nitride material was employed as it meets the requirements for the tool high-temperature stability and strength. However, the tool material cost was excessively high, creating a barrier to welding high-temperature materials.[7] Miyazawa et al.[8] used an iridium-based alloy tool for FSW. This alloy has a high melting point, good mechanical qualities, and it is resistant to oxidation at high temperatures. But, the main drawback is the lack of availability of the material to be commercialized.

*Corresponding author's e-mail:
sunmetly@gmail.com (Sundar raju Govindaraj)

Table 1: Chemical composition of the base metal (*w*/%)

Material/ elements	C	Cr	Ni	Mn	Si	Mo	S	P	Cu	Co	V	Fe
AISI 304	0.06	18.4	8.09	0.84	0.23	0.22	0.001	0.042	0.294	0.186	0.062	Rem

Lakshminarayan et al.[9] investigated the FSW of AISI 304 using a surface-coated tool. According to the results, the atmospheric plasma sprayed (APS) coatings exhibited inadequate shear and bond strength, causing premature failure during the plunging stage. Raghunathan et al.[10] investigated the deterioration of different tool materials in FSW, finding that among tungsten alloy tools the one with 99 % of W and 1 % of La_2O_3 maintains good properties at high temperatures with negligible tool debris and base-material degradation. These authors focused on the tool material and geometry required for AISI 304 welding. The FSW process is controlled by welding-process parameters such as the tool material, tool shape, welding speed, rotational speed and axial forces. Abbasi et al.[11] found that rising the tool traverse speed enhances the weld nugget size and reduces incomplete root penetration. Ahmed et al.[12] showed that an increased FSW speed results in a higher grain-size reduction and improved hardness values. Guo et al.[13] maintained that thin sheets are always prone to a heat input, and that the pin wear is pretty high when the welding speed is too slow. Plaine et al.[14] maintained that the FSW process generates fine grains with good mechanical properties with a low heat input. Mishra et al.[15] stated that the material flow during friction stir welding is quite complex as it depends on the tool geometry, process parameters and material to be welded.

The tool rotational speed has a direct effect on the thermal history, frictional heat stirring, oxide layer breaking, and mixing of the materials of FSW joints. Jabbari et al.[16] found that increasing the rotation speed results in an increase in the grain size in the nugget zone. Ko et al.[17] found that the tensile strength and hardness of the stir zone increased as the tool rotational speed increased. Li et al.[18] found that when the rotational speed increases, the hardness of the heat-affected zone decreases gradually, and the hardness of the stir zone increases. For this reason, this study will focus on the effect of the tool rotation speed on the mechanical and microstructural properties of AISI 304 steel using a W-La_2O_3 alloy tool.

2 EXPERIMENTAL PART

The base material for this experiment was a cold-rolled and annealed AISI 304 stainless-steel sheet with a thickness of 3 mm. A spectrum analysis was performed in three locations to determine the alloy composition, with the average values reported in **Table 1**.

A semi-automatic friction stir welding machine with a spindle speed of 2000 min^{-1} and a Z axial force of 15 kN, and a Rexroth controller with a liquid-cooled tool holder machine were employed in this operation. The W-alloy tool utilized with this technique was a cylindrical tool with a shoulder diameter of 25 mm, a probe diameter of 12 mm and a conical-pin length of 2.9 mm. The FSW joints were tested at various tool rotational speeds of (600, 700, 800, 900 and 1000) min^{-1}, with a constant welding speed of 40 mm/min and a 15 kN axial load. ASTM E8M-04 was used to prepare tensile specimens. Experiments were performed in a computer-controlled UTM machine (M-30 model). Charpy impact specimens were made according to ASTM E23-06. To examine the impact toughness of the samples (AIT-300-EN type), an impact test machine with a 300 J capacity was used. The specimens were produced following the ASTM E190-03 specifications and tested in a compression testing machine with a load capacity of 400 kN (model number: TUE-CN-400). Microhardness tests were carried out on the base metal, weld metal and TMAZ, using a Vickers microhardness testing machine (model number: Qness Q10A+) with an applied load of 500 gf and a dwell time of 10 s.

3 RESULTS AND DISCUSSIONS

FSW joints were prepared at various tool rotational speeds of 600 min^{-1} to 1000 min^{-1} with intervals of 100 min^{-1}. Surface and volumetric defect-free weld joints were achieved at tool rotational speeds of

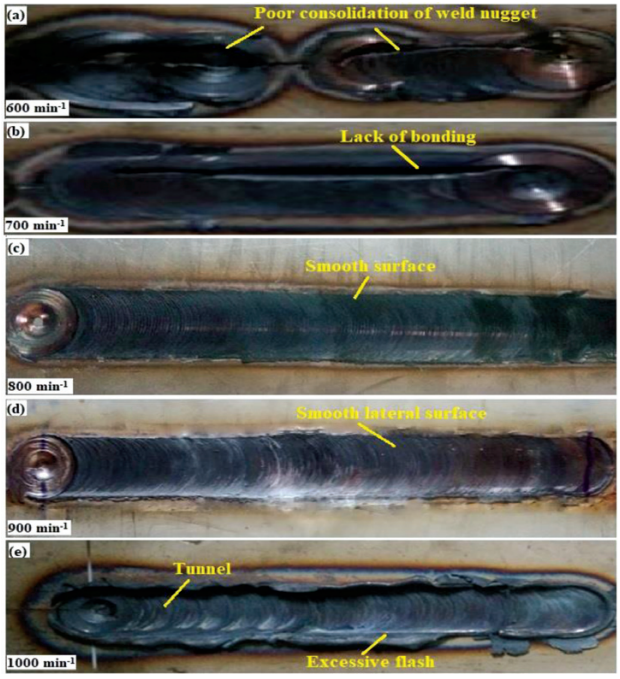

Figure 1: FSW joints at various tool rotational speeds

800 min^{-1} and 900 min^{-1} (**Figures 1c** and **1d**). The joint made at a tool rotational speed of 600 min^{-1} exhibits poor consolidation of the weld nugget defect due to a low temperature and low material flow in the stir zone. The weld produced at 700 min^{-1} exhibits a lack of bonding defect because of a low frictional force, which created an insufficient heat input. The welds in the stir zone consist of smooth onion rings at 800 min^{-1} and 900 min^{-1}, indicating a proper plastic flow of the material and adequate heat generation during welding. Finally, at a tool rotational speed of 1000 min^{-1}, excessive flash generation and tunnel flaws are observed. This is due to the excess heat input and high tool shoulder pressure. As a result of the above, a low rotational speed and high rotational speed are not advisable. The optimum tool rotational speed should be used to attain flaw-free welds. Thus, the tool rotational speeds of 800 min^{-1} and 900 min^{-1} resulting in sound weld joints were selected for further investigations.

3.1 Tensile test

Stress-strain curves and transverse tensile characteristics of the base metal (BM) and FSW joints are shown in **Figure 2**. The yield strength (YS) and ultimate tensile strength (UTS) of the base metal are 343 MPa and 674 MPa, respectively. The joint yield strength at the tool rotational speeds of 800 min^{-1} and 900 min^{-1} are greater than that of the base metal in both cases. The average of three specimen yield strengths (YS) was measured at 351 MPa and 362 MPa. The grain refinement and work hardening effect in the weld zone were the key reasons for the increased yield strength. The average of the ultimate tensile strength was measured at 575 MPa and 647 MPa when the tool rotational speeds were 800 min^{-1} and 900 min^{-1}. At the 800 min^{-1} and 900 min^{-1} tool rotational speeds, the joint efficiency was estimated to be 85 % and 96 % with regard to the base metal. The base metal melted more when the coefficient of friction between the tool and the parent material decreased. This caused a stirring action, lowering the joint tensile strength.

The tensile-test results indicated that the tool rotational rates of 800 min^{-1} and 900 min^{-1} provide enough heat input and a defect-free weld joint. The location of fracture was seen in the stir zone and the TMAZ of the advancing side at the 800 min^{-1} tool rotational speed. The advancing-side gradient of velocity was high when compared to the retreating side. A fracture was found in the stir zone, adjacent to the TMAZ on the advancing side, with a tool rotational speed of 800 min^{-1}. When compared to the retreating side, the advancing side had a higher velocity gradient. Under the influence of the pin, the stir zone exhibits significant plastic deformation, producing small grains through dynamic recovery and recrystallization and leading to an increased hardness and tensile strength as shown by Li et al.[19,20] According to the fine-grain strengthening theory, small grains in the stir zone increase the weld strength.

3.2 Impact test

The impact toughness of the base metal and FSW joints is shown in **Figure 3**. The test results show that the base-metal impact toughness is 64 J at room temperature. The welded-metal impact-toughness values obtained at the tool rotational speeds of 800 min^{-1} and 900 min^{-1} are 44 J and 48 J. Comparing the base metal and welded metal, we find that the toughness value slump rapidly at both tool rotational speeds. This is due to the tool wear during the FSW process. A similar result was described by G. Sundar raju et al.[21] The addition of tungsten particles to the tool-wear debris reduces the ductility and toughness of the particles in the pin-affected zone. Lakshminarayan et al.[22] report that the presence of tool debris at the bottom of the stir zone may be the reason for the reduction in ductility and toughness of a friction-stir-welded joint compared to the base metal.

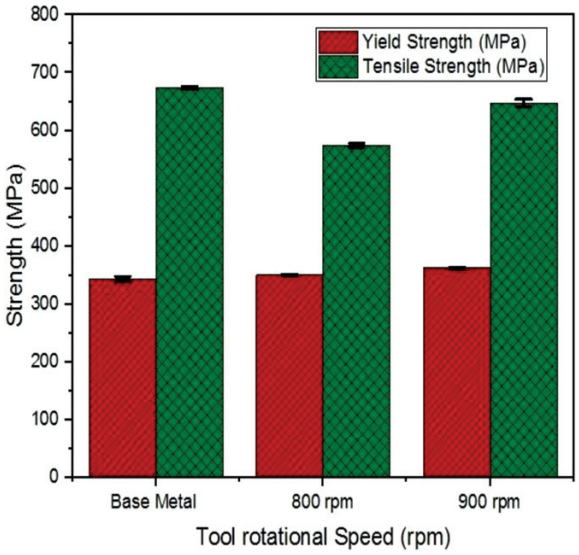

Figure 2: Transverse tensile properties of BM and FSW joints

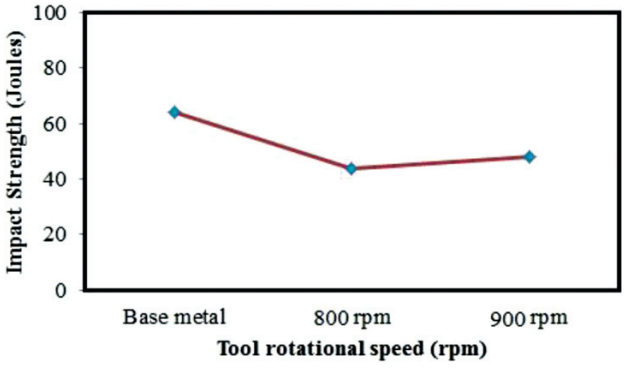

Figure 3: Impact toughness properties of BM and FSW joints

3.3 Bend test

The three-point guided bend test result helps to determine the ductility of the weld on both the surface and root side (bottom side). This test was performed in the transverse direction on the FSW joints. The compressive strength of the base metal and FSW joints is shown in **Figure 4**. The base-metal compressive-strength value is 58.6 N/mm^2. It is estimated that at the tool rotational speeds of 800 min^{-1} and 900 min^{-1} the face-side weld-metal compressive-strength values are 46.4 N/mm^2 and 53.9 N/mm^2 while the root-side weld-metal compressive-strength values are 44.5 N/mm^2 and 52.9 N/mm^2. The results of the face bend and root bend tests indicate that the 800 min^{-1} joint has a lower compressive strength than the base metal. However, the FSW joints show satisfactory ductility in both bend tests.

3.4 Microhardness test

The microhardness of the butt joints obtained at 800 and 900 min^{-1} was tested in the transverse direction, at the center, and the values are shown in **Figure 5**. The average base-metal hardness is 223 ± 5 HV. All the defect-free weld joints show a substantial increase in the hardness when compared to the base metal. With the tool rotational speed of 800 min^{-1}, the hardness of the stir zone varies from 224 HV to a peak hardness of 243 HV in the centerline, and the average hardness is 235 ± 5 HV. Similarly, with the tool rotational speed of 900 min^{-1}, a high hardness of 294 HV is observed in the stir zone, and the average hardness is estimated to be 278 ± 5 HV, which is greater than the base-metal and TMAZ hardness values. The hardness in the TMAZ is higher than that of the base metal and lower than that of the stir zone. In the TMAZ, high dislocation and subgrain boundaries tend to improve the hardness as reported by Guo et al.[23] The hardness profile increases from the TMAZ to the center of the stir zone on both the advancing and retreating sides. FSW welds have higher hardness than the base metal due to the high density of dislocations and continuous dynamic recrystallization, resulting in fine grains in the stir zone.

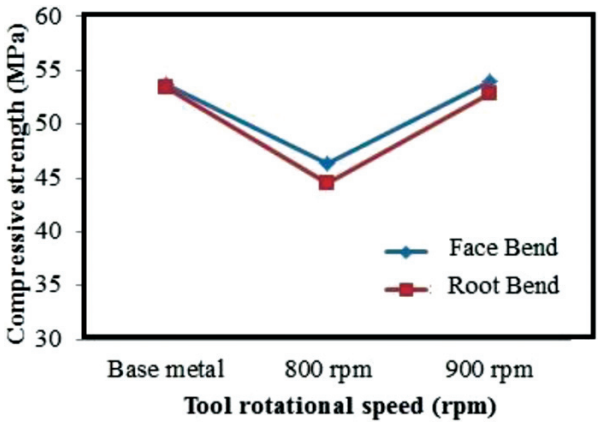

Figure 4: Compressive strength properties of BM and FSW joints

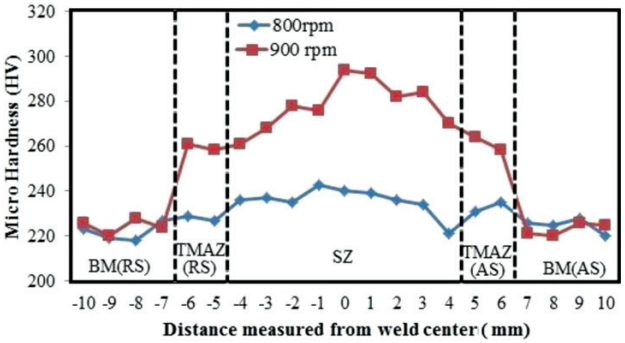

Figure 5: Transverse microhardness surveys of FSWs at 800 min^{-1} and 900 min^{-1}

3.5 Weld macrostructure

In **Figure 6**, the tool rotational speed of 800 min^{-1} was observed to create a sound metal deposition, layer by layer, on the advancing side (AS). This is because the material flows from the advancing side to the retreating side (RS), requiring more energy to flow from one side to the other. Similarly, a defect-free weld joint was formed at the tool rotational speed of 900 min^{-1}, with U-shaped shear bands in the stir zone and near the thermo-mechanically affected zone (TMAZ). The U-shaped shear band at the stir zone (SZ) was observed by Shashikumar et al.,[24] indicating an adequate heat generation due to a consistent material flow and enhanced material coalescence.

3.6 Weld microstructure

The base material has an austenite grain structure (γ-Fe) with a low density of dislocations. Annealed twin boundaries are also observed in some grains. The average grain size of the BM is about 8 μm. The parent-metal and welded-metal microstructures are shown in **Figure 7**. There are three distinct zones in the microstructures: the base metal (BM), thermomechanically affected zone (TMAZ) and stir zone (SZ). The grain structure in the stir zone is generally equiaxed, and the stir zone has a higher dislocation density than the base metal. The average grain size in the SZ is 7.0 μm, which is slightly smaller than that of the BM. The microstructures from **Figures 7a** and **7b** show the BM and SZ of the shoulder and pin-influenced region. Small equiaxed grains are observed throughout the SZ. This zone is refined compared

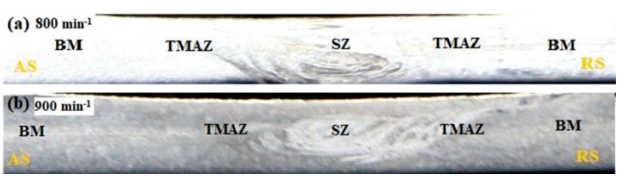

Figure 6: Macrostructures of FSW joints at 800 min^{-1} and 900 min^{-1}

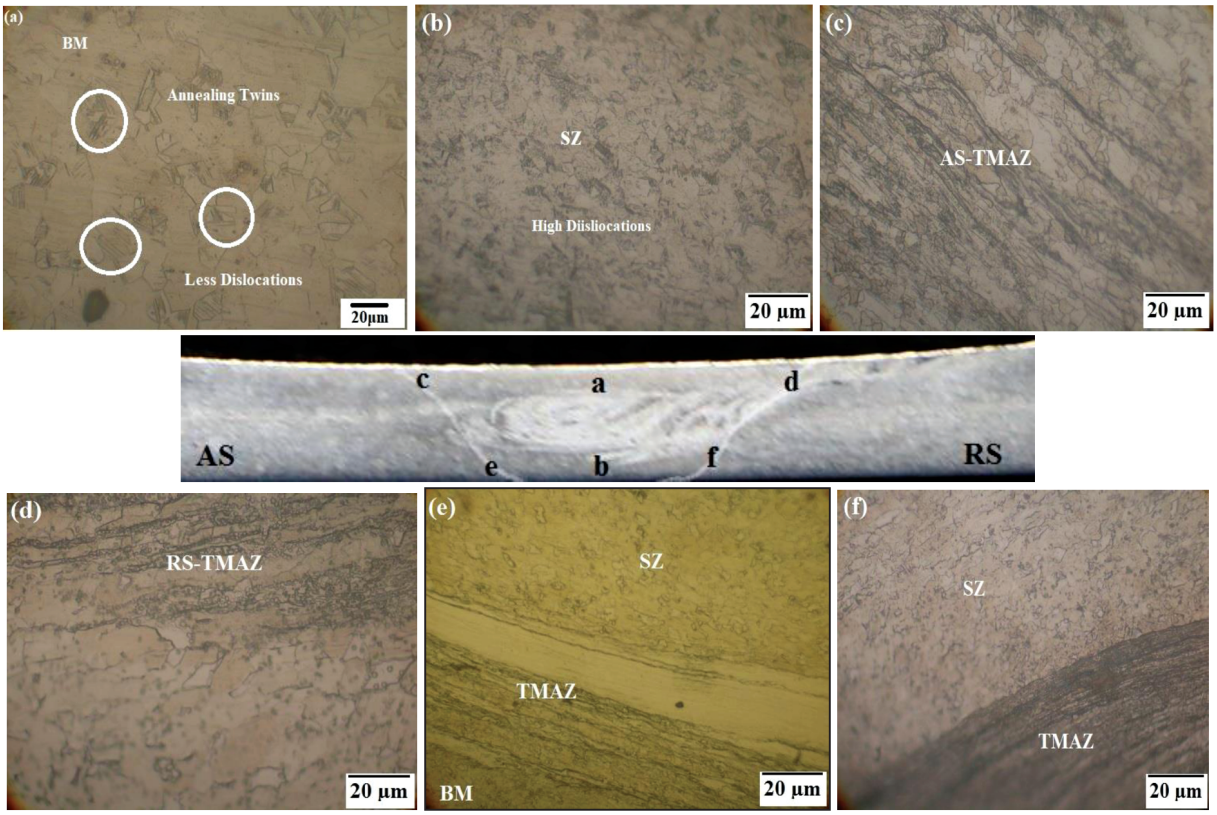

Figure 7: Optical micrographs of FSW joints

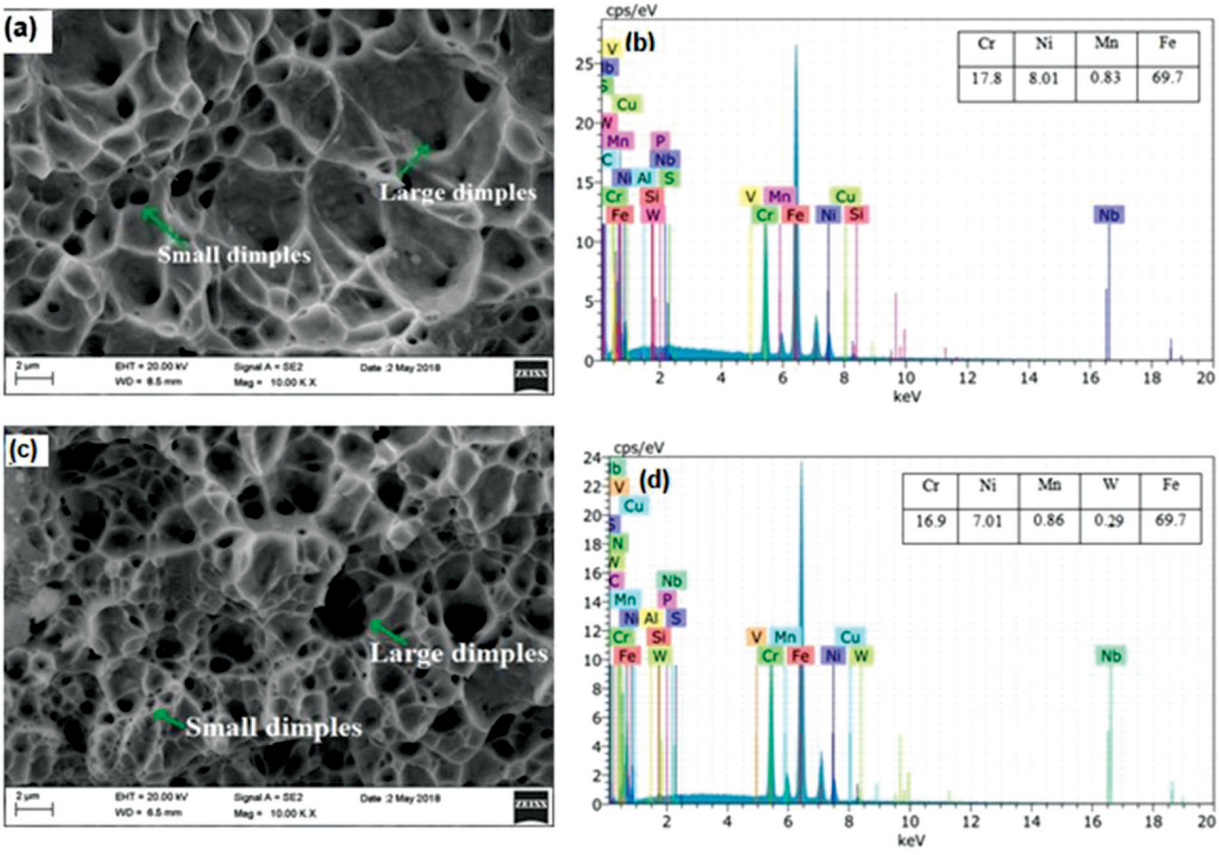

Figure 8: Fractographs and EDS of the tensile tests: a), b) base metal, c), d) weld metal

with the base metal, exhibiting an equiaxed recrystallized grain structure. Further, no annealed twin grains found in the SZ are completely reoriented by the stirring action of the tool. The combined effect of thermal and mechanical loads forms the TMAZ. **Figures 7c** and **7d** display the TMAZs of the advancing and retreating sides. Because of the material flow process, the advancing side of the figure shows a most severe displacement. Furthermore, the tool advancing side causes more plastic deformation than the retreating side due to the shear force. **Figures 7e** and **7f** depict the microstructures of the SZ and TMAZ interface regions of the advancing and retreating sides. The TMAZ at the bottom of the pin-influenced region is smaller than the TMAZ-AS&RS of the shoulder-influenced region and pin-influenced region due to a higher cooling rate. Furthermore, similar microstructure properties were observed in a 304 ASS friction-stir weld by Park et al.[25] The microstructure at the bottom of the advancing side of the stir zone is relatively more sensitive to etching than the other regions; it consists of austenite and ferrite phases. A microstructural study exposes the quality of weld joints since the microstructures of weld joints have a significant impact on their mechanical characteristics, as shown by Yan et al.[26]

3.7 Fracture surface analysis – a tensile test

The fracture surfaces of the base-metal and weld-metal tensile specimens are shown in **Figure 8**. The displayed fractograph in **8a** invariably consists of dimples with a large void volume fraction. Small or large dimples and microvoids can be seen in the images, indicating that the tensile specimens failed in a ductile manner under the action of a uniaxial tensile load. The fracture surface of the tensile specimen of the welded metal is shown in **Figure 8c**. The fractograph shows a great amount of small or large dimples and microvoids. Comparing the base-metal and welded-metal fractographs, finer dimples are found in the FSW joint. In addition, parabolically shaped fine microvoids are present in the welded fracture surface.

Figures 8b and **8d** depict the tensile-test SEM-EDS analysis of the base metal and weld metal, used to analyze the energy spectrum to determine the specific elements. In the FSW process, light etching features occur between the tool and base material. These characteristics are the result of high-pressure mechanical stirring and the transfer of the tool material to the base material. In the shown EDS photograph no substantial W-tool debris is observed, so inclusion occurs in the weld joints.

3.8 Fracture surface analysis – an impact test

The fracture surfaces of the base-metal and weld-metal impact specimens are shown in **Figure 9**. **Figure 9a** shows a typical SEM fractograph of the impact-test image of the base metal. The fractograph displays a fibrous appearance and substantial deformation before the fracture, indicating ductile fracture qualities. Further, the void coalescence results in the development of a shear lip, and the microvoids are responsible for a higher self-energy fracture. **Figure 9b** depicts the SEM-EDS analysis of the base metal. According to its result, in the base metal, Ni and Mn are predominantly present, following the Cr content, which acts as the austenite stabilizer.

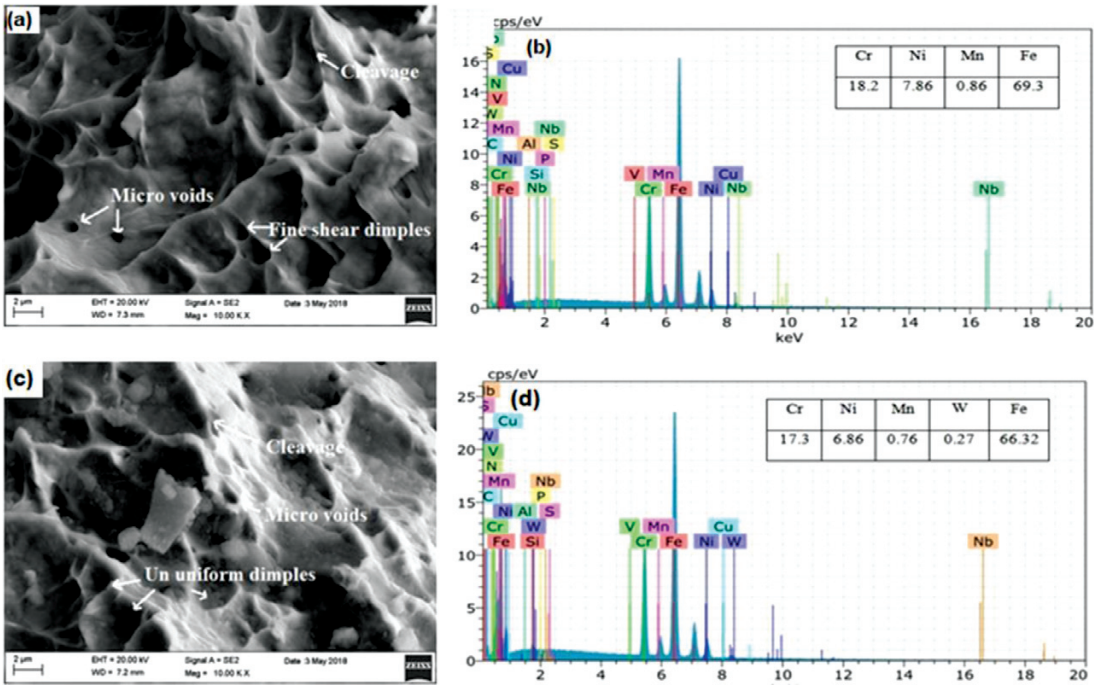

Figure 9: Fractographs and EDS of the impact tests: a), b) base metal, c), d) weld metal

Figure 9c shows a typical SEM fractograph of the impact-test image of the FSW joint. On the fractograph, the microvoids and non-uniform dimples are signs of a ductile fracture with a high energy mode. Moreover, shear cleavage and minor broken grains inside the dimples are also found. In comparison to the base metal, the grain size and void size increased significantly, being the origin of the poor toughness of the material. **Figure 9d** depicts the SEM-EDS analysis of the weld metal. The result explains the composition of the weld metal in the fracture area. It is noticed that the least amount of tungsten inclusion is present in the weld metal, resulting in the reduced toughness of the weld metal. In addition, sufficient levels of toughness and tensile strength are attained at the welding speed of 900 min^{-1}.

4 CONCLUSION

Friction stir welding of AISI 304 austenitic stainless steel was effectively accomplished at an axial load of 15 kN, constant welding speed of 40 mm/min and tool rotation speeds of 800 min^{-1} and 900 min^{-1}.

It was observed that increasing and decreasing the tool rotational speed influenced the quality of the welding.

FSW produced sound welds with no cracks or cavities at tool rotational speeds of 800 min^{-1} and 900 min^{-1}.

Welding process parameters directly influenced mechanical properties, including a maximum tensile strength of 647 MPa and compressive strength of 53.9 N/mm^2, obtained at the welding speed of 900 min^{-1}.

The microhardness of the base metal was 221 ± 5 HV. At the tool rotation speed of 900 min^{-1}, the stir zone microhardness reached a maximum of 233 ± 5 HV.

The base-metal impact toughness was 64 J at room temperature. The welded-metal impact toughness values were 44 J and 48 J, obtained at the tool rotational speeds of 800 min^{-1} and 900 min^{-1}.

SEM results showed the size and dimple distribution for the welded tensile specimen, indicating characteristics of a ductile fracture.

It was determined that the problem of excessive grain growth and sigma-phase formation associated with fusion welding can be overcome with FSW.

5 REFERENCES

[1] W. M. Thomas, Friction stir butt welding, International Patent No. PCT/GB92/02203, England 1991

[2] F. Zhi-hing, H. Di-qiu, W. Hong, Friction stir welding of aluminum alloys, J. Wuhan Univ. Technol. – Mat. Science Edition, 19 (**2004**), 61–64, doi:10.1007/BF02838366

[3] S. Benavides, Y. Li, L. Murr, D. Brown, J. McClure, Low-temperature friction-stir welding of 2024 aluminum, Scripta Materialia, 41 (**1999**) 8, doi:10.1016/S1359-6462(99)00226-2

[4] https://www.assda.asn.au/43-applications/marine/170-corrosion-resistance-in-marine-environments, 10.10.1996

[5] B. C. Gerwick Jr, Construction of marine and offshore structures, 3rd edition, CRC Press, United States of America 2007, 8493–3052

[6] D. G. Mohan, C. Wu, A Review on Friction Stir Welding of Steels, Chinese Journal of Mechanical Engineering, 34 (**2021**) 1, 1–29, doi:10.1186/s10033-021-00655-3

[7] Y. N. Zhang, X. Cao, S. Larose, P. Wanjara, Reviews of tools for friction stir welding and processing, Canadian Metallurgical Quarterly, 51 (**2012**) 3, 250–261, doi:10.1179/1879139512Y.0000000015

[8] T. Miyazawa, Y. Iwamoto, T. Maruko, H. Fujji, Friction stir welding of 304 stainless steel using Ir based alloy tool, Science and Technology of Welding and Joining, 17 (**2012**) 3, 207–212, doi:10.1179/1362171811Y.0000000096

[9] A. K. Lakshminarayanan, C. S. Ramachandran, V. Balasubramanian, Feasibility of surface-coated friction stir welding tools to join AISI 304 grade austenitic stainless steel, Defense Technology, 10 (**2014**) 4, 360–370, doi:10.1016/j.dt.2014.07.003

[10] S. R. Nathan, V. Balasubramanian, S. Malarvizhi, A. G. Rao, An investigation on metallurgical characteristics of tungsten based tool materials used in friction stir welding of naval grade high strength low alloy steels, International Journal of Refractory Metals and Hard Materials, 56 (**2016**), 18–26, doi:10.1016/j.ijrmhm. 2015.12.005

[11] M. A. Gharacheh, A. H. Kokabi, G. H. Daneshi, B. Shalchi, R. Sarrafi, The influence of the ratio of "rotational speed/traverse speed" (ω/v) on mechanical properties of AZ31 friction stir welds, International Journal of Machine Tools and Manufacture, 46 (**2006**) 15, 1983–1987, doi:10.1016/j.ijmachtools.2006.01.007

[12] M. M. Z. Ahmed, B. P. Wynne, J. P. Martin, Effect of friction stir welding speed on mechanical properties and microstructure of nickel based super alloy Inconel 718, Science and Technology of Welding and Joining, 18 (**2013**) 8, 680–687, doi:10.1179/1362171813Y.0000000156

[13] G. Guo, Y. Shen, Frictions stir welding of dissimilar stainless steels: evaluation of flow pattern, microstructure and mechanical properties, Materials Research Express, 6 (**2019**) 5, 056510, doi:10.1088/2053-1591/ab015b

[14] A. H. Plaine, N. G. D Alcântara, Prediction of FSW defect-free joints of AISI 304 austenitic stainless steel through axial force profile understanding, Materials Research, 17 (**2014**), 1324–1327, doi:10.1590/ 1516-1439.292714

[15] R. S. Mishra, Z. Y. Ma, Frictions stir welding and processing, Materials Science and Engineering: R: Reports, 50 (**2005**) 1–2, 1–78, doi:10.1016/j.mser.2005.07.001

[16] M. Jabbari, C. C. Tutum, Optimum rotation speed for the friction stir welding of pure copper, International Scholarly Research Notices, (**2013**), doi:10.1155/2013/978031

[17] Y. J. Ko, K. J. Lee, K. H. Baik, Effect of tool rotational speed on mechanical properties and microstructure of friction stir welding joints within Ti–6Al–4V alloy sheets, Advances in Mechanical Engineering, 9 (**2017**) 8, 1687814017709702, doi:10.1155/2013/978031

[18] Y. Li, D. Sun, W. Gong, Effect of tool rotational speed on the microstructure and mechanical properties of bobbin tool friction stir welded 6082-T6 aluminum alloy, Metals, 9 (**2019**) 8, 894, doi:10.3390/met9080894

[19] J. Li, X. Liu, G. Li, P. Han, W. Liang, Characterization of the microstructure, mechanical properties, and corrosion resistance of a friction-stir-welded joint of hyper duplex stainless steel, Metals 7 (**2017**) 4, 138, doi:10.3390/met7040138

[20] H. B. Li, Z. H. Jiang, H. Feng, S. C. Zhang, L. Li, P. D. Han, J. Z. Li, Microstructure, mechanical and corrosion properties of friction stir welded high nitrogen nickel-free austenitic stainless steel, Materials & Design, 84 (**2015**), 291–299, doi:10.1016/j.matdes.2015.06.103

[21] G. Sundar raju, K. Sivakumar, S. R. Nathan, Influence of tool rotational speed on the mechanical and micro structural properties of AISI 316 Austenitic stainless steel friction stir welded joints, Materials Research Express, 6 (**2020**) 12, 1265d7, doi:10.1088/2053-1591/ab6248

[22] A. K. Lakshminarayanan, V. Balasubramanian, M. Salahuddin, Microstructure, tensile and impact toughness properties of friction

stir welded mild steel, Journal of Iron and Steel Research International, 17 (**2010**) 10, 68–74, doi:10.1016/S1006-706X(10)60186-0

[23] R. Guo, Y. Huang, W. Zhang, W. Guan, Microstructures and mechanical properties of thin 304 stainless steel sheets by friction stir welding, Journal of Adhesion Science and Technology, 32 (**2018**) 12, 1313–1323, doi:10.1080/01694243.2017.1409064

[24] S. S. Kumar, N. Murugan, K. K. Ramachandran, Identifying the optimal FSW process parameters for maximizing the tensile strength of friction stir welded AISI 316L butt joints, Measurement, 137 (**2019**), 257–271, doi:10.1016/j.measurement.2019.01.023

[25] S. H. C Park, Y. S. Sato, H. Kokawa, K. Okamoto, S. Hirano, M. Inagaki, Microstructural characterization of stir zone containing residual ferrite in friction stir welded 304 austenitic stainless steel, Science and Technology of Welding and Joining, 10 (**2005**) 5, 550–556, doi:10.1179/174329305X46691

[26] J. Yan, M. Gao, X. Zeng, Study on microstructure and mechanical properties of 304 SS joints by TIG, laser and laser-TIG hybrid welding, Optics and Lasers in Engineering, 48 (**2010**) 4, 512–517, doi:10.1016/j.optlaseng.2009.08.009